CPT-Based Liquefaction Resistance of Clean and Silty Sands: A Drainage conditions Based Approach

Nurhan Ecemis (nurhanecemis@iyte.edu.tr)
Izmir Institute of Technology: Izmir Yuksek Teknoloji Enstitusu
Mehmet Murat Monkul
Yeditepe University: Yeditepe Universitesi
Yunus Emre Tütüncü
Yeditepe University: Yeditepe Universitesi
Mustafa Sezer Arik
Izmir Institute of Technology: Izmir Yuksek Teknoloji Enstitusu

Research Article

Keywords: Liquefaction resistance, cone penetration test, cyclic simple shear test, sand, silt, coefficient of consolidation, relative density

Posted Date: March 10th, 2022

DOI: https://doi.org/10.21203/rs.3.rs-1427044/v1

Abstract

The cone penetration test-based simplified liquefaction triggering evaluations are largely based on linking liquefaction manifestations in the field to cone penetration resistance. These relationships are interpreted in such a way that for given penetration resistance, the liquefaction resistance increases as non-plastic fines content (FC) increases. However, several studies have indicated discrepancies in this relationship. Hence, there is a lag in rational scientific understanding of this observation. In this study, an experimental research program was undertaken to investigate the CPT-based liquefaction assessment by considering the effects of drainage conditions on the relationship between CPT resistance and liquefaction resistance. First, clean sand and silty sands having 5, 15, and 35% FC were tested at different relative densities by stress-controlled cyclic direct simple shear (CDSS) tests to investigate cyclic resistance of silty sand with varying amounts of non-plastic fines. Then, a set of tests involving piezocone penetration (CPTu), seismic CPTu (SCPTu), and direct push permeability (DPPT) were undertaken in a large-scale box filled with the same soils used in the CDSS tests. The large-scale test results quantified the effect of drainage conditions (coefficient of consolidation) on cone penetration resistance. Finally, by combining the CDSS and CPTu test results, an alternative CPT-based liquefaction resistance relationship was proposed by considering the effects of drainage conditions.

1. Introduction

Over the past three decades, researchers have observed that non/low plastic silty sands are commonly involved in liquefaction, and in some cases even silts could liquefy [e.g., 1,2]. Therefore, there have been many laboratory-based studies investigating the liquefaction resistance of silty sands. Many laboratory studies indicated that cyclic liquefaction resistance decreased with increasing FC up to threshold value (btwn. 15% and 40%) [3–10]. Although, the opposite trend (i.e., an increase in cyclic liquefaction resistance with increasing FC) was reported by several other studies [6, 11–13]. Meanwhile, some other studies involve results which denote a temporary increase in the cyclic liquefaction resistance up to a low FC (e.g., 6%), followed by a decrease in liquefaction resistance with further increasing fines content [14–16]. In a recent study, Monkul et al. [16] proposed a new equation on cyclic liquefaction resistance of silty sands, which considers the combined effect of fines content with uniformity coefficient (i.e. gradation). Nevertheless, the problem of fines' effect on liquefaction is complex, and one of the possible reasons for different observations in the laboratory-based studies mentioned above is the density index parameter (e.g., similar void ratio, inter-granular void ratio, or relative density) used to compare the liquefaction resistances [17–20]. It should be reminded that the fines' plasticity makes the problem more complicated [21–23]. The mentioned studies above [btwn. 3 to 20] typically investigated the effect of non-plastic fines, except the three [11, 13, 16], which had silts with plasticity index of 3 and 11, respectively.

As summarized by Youd et al. [24], the liquefaction potential of sandy soils can be determined by several in-situ tests, including the standard penetration test (SPT), cone penetration test (CPT), and shear wave velocity (V_s) test. When the commonly used CPT-based liquefaction assessment chart—developed by Robertson and Wride [25]—is considered, the chart is documented in the form of normalized cone

penetration resistance (qc1N) versus cyclic resistance ratio ($CRR_{7.5} = \tau_{ave}/\sigma_{vo}'$), applicable for an earthquake magnitude of 7.5. In order to account for the variations in the magnitude of an earthquake, $(CRR)_{7.5}$ requires to be corrected by the scaling factor [24]. In the conventional liquefaction assessment charts, there are three demarcation curves that correspond to three different fines content values of FC ≤ 5%, FC = 15%, and FC = 35%. These demarcation curves were determined by the CPT tests and the field liquefaction observations at different sites, based on the indication of liquefaction (e.g., sand boils, lateral spreading, and bearing capacity loss) during the earthquakes [25]. It has become apparent that liquefaction resistance determined in this manner depends on the grain size distribution characteristics, involving fines content of the soil for a given q_{c1N}. Particularly, the widely used liquefaction assessment chart implies that for the same q_{c1N} the liquefaction resistance increases progressively up, apparently, to a fines content of about 35%, as the curves seem to shift to the left with increasing FC.

Several researchers have studied the effects of fines on liquefaction screening using the cone penetration resistance [e.g., 14, 26–30]. Some studies showed an increase in CRR with increasing FC at a given q_{c1N} [26, 27, 29, 30]. Juang et al. [26] developed a CPT-based empirical equation for CRR using a neural network methodology on CPT data and field liquefaction performance observations during historical earthquakes. Their study resulted in a similar chart with the widely used CPT-based correlations proposed by Robertson and Wride [25]. Huang et al. [27] performed cone penetration chamber tests and cyclic triaxial tests on two different sand types with various FC and relative densities. Their results showed that the CRR-q_{c1N} correlation consistently fell below the accepted correlations.

Moss et al. [29] found significantly different correlations from that of Robertson and Wride's [25]. There are also some studies that concluded that CRR decreases with the increase of FC at a given qc1N (i.e., the curves seem to shift to the right with increasing FC). For instance, Carraro et al. [14] carried out cyclic triaxial tests and cavity expansion analysis for clean and silty sands at various relative density values, developing a CRR-q_{c1} relationship. The liquefaction assessment charts that Carraro et al. [14] proposed implies that the higher fines content in sand tends to decrease its liquefaction resistance at a given cone penetration resistance. On the other hand, Kokusho et al. [28] found a single correlation between the CRR and the cone penetration resistance despite the large differences in relative density or FC. These observations show that it is not clear whether the fines reduce the cone penetration resistance or increase the liquefaction resistance. Despite its importance in engineering design, further research is still needed for a rational understanding of the relationship between cone penetration resistance and cyclic resistance of clean and silty sands. Hence, the successful application of CPT-based liquefaction assessment chart methods require detailed insight regarding the effects of non/low plastic fines on the relationship between liquefaction resistance of sands and their CPT resistance.

It needs to be restated that clean and silty sands have different drainage conditions (permeability and coefficient of consolidation) at different relative densities, which influences the cone penetration resistance [31, 32]. Relatively recently, a non-dimensional parameter T (= vd/c_h) has been utilized to study the effect of the coefficient of consolidation (c_h), the rate of cone penetration (v), and cone diameter (d)

on the measured CPT resistance, as well as the excess pore water pressure during penetration of the cone into the soil [33–37]. Two soils having similar CRR may have different FCs, as well as different permeabilities, compressibilities, and coefficients of consolidation. In fact, Robertson and Wride [25] stated that for a given CRR, silty sands have lower CPT resistance than the clean sands in liquefaction charts because of having greater compressibility and smaller permeability (k) than the clean sands.

In order to establish direct correlations between cone penetration resistance and CRR considering the effect of fines and drainage conditions, this study involves systematic laboratory research, in which piezocone penetration (CPTu), seismic CPTu (SCPTu), and direct push permeability (DPPT) tests, and subsequent cyclic direct simple shear (CDSS) tests were carried out on the same soils by changing D_r and FC. The CRR values obtained from CDSS experiments were correlated with qc1N, obtained from several large-scale CPTu tests at the corresponding relative densities. The first part of this paper builds on the results on the effects of relative density and FC on liquefaction resistance, permeability, and consolidation characteristics. The second part implements this understanding to determine how FC and normalized penetration rate (drainage conditions) affect cone penetration resistance and their relationship to liquefaction resistance. Finally, by combining the CDSS and CPTu test results, a liquefaction assessment chart is proposed, where the relationship between CPT resistance and liquefaction resistance is plotted considering the effects of drainage conditions. With such an approach, the influence of fines on liquefaction resistance is also inherently considered in the proposed CPT chart.

2. Soil Properties

Clean sand and non-plastic silt were used in the experimental portion of this study. The base sand was obtained from the Urla district in the city of Izmir. The non-plastic silt was a naturally formed soil from the Babaeski region of Kırklareli. The sand and silt consisted of mainly quaternary sediments which consists of alluvial soils transported by the rivers. Only the minus No 200 portion (< 0.075mm) of the silt, obtained by wet sieving, was used in the experiments. Several sand-silt mixtures were prepared by mixing sand with non-plastic fines (silt) at contents of 5, 15, and 35% by dry weight. Figure 1a shows the grain size distribution curves of clean sand and sand-silt mixtures used in both piezocone penetration tests (CPTu) and cyclic direct simple shear tests. The index properties of clean sand and sand-silt mixtures are listed in Table 1. Based on the unified soil classification scheme [38], the clean sand and the sand-silt mixtures were defined as poorly graded sand (SP) and silty sand (SM), respectively. The microscopic view of silt and sub-angular silica sand particles is shown in Fig. 1b.

The change of maximum (e_{max}) and minimum (e_{min}) void ratios with FC of different silts are plotted in Fig. 2a. As the silt content increases, the e_{max} and e_{min} values of these samples are reduced to about 30 to 35% FC. The limit void ratios for each silty sand sample were obtained by the method proposed by Lade et al. [39], using a 2000 ml calibrated graduated cylinder. Lade et al. [39] explained the experimental procedure, repeatability, and other details of their method, which would not be repeated here. However, some general issues regarding extreme void ratio determination should be reminded here, such as the limitation of most standards for determining e_{max} and e_{min}, which originally intended for sands up to a

certain amount of fines content. For example, ASTM procedures were intended for sand with FC up to 15%, while the Japanese Geotechnical Society's procedures were intended for sand with less than 5% FC [40]. Consequently, the fines content range investigated in this study is technically greater than what is allowed by many standards. Therefore, a non-standard procedure [39] was chosen in this study, which had been successfully used for obtaining the e_{max} and e_{min} of various silty sands in the literature that have quite a wide fines content range [16, 19–21, 41–43].

Figure 2b shows the variation of k with various D_r at different fines content of 0, 5, 15, and 35% for clean and silty sands used in the experiments. For soils having FC = 0% and 5%, the k values were obtained from constant head permeability tests [44]. Additionally, falling head permeability tests [44] were performed for soils having FC = 15 and 35%, at a range of different relative density values. The relationships between k and D_r are shown by the solid trend curves, presented in Fig. 2b, for sand at different FCs between 0% and 35%.

The results show that the permeability of clean and silty sand are not the same, even at the same relative density, which is an expected observation due to the changes in grain and pore size distributions. The permeability of saturated sand containing 5% silt is roughly less than a half order of magnitude smaller than the permeability of clean sand; however, both curves (0% and 5% FC) come close to each other as soils become loose (i.e., $D_r \approx 25\%$). The permeability of saturated sand containing 15% silt is almost two orders of magnitude smaller than the permeability of clean sand. The significant drop in the k value with an increase of FC towards 15% is mainly because of the reduced pore size within the overall grain matrix. The measured k values of clean sand and 5% are influenced relatively less by the change in relative density within the studied range; although a modest decrease (i.e., less than half an order) can be observed with an increasing D_r. However, the sensitivity of k to D_r is more noticeable at FC = 15% and 35% (i.e., k decreases rapidly as D_r increases towards medium-dense to dense states). Hence, for a given fines content (at FC = 15% or 35%), the k could range within one order of magnitude, depending on the relative density.

3. Experimental Research Program

3.1 Cyclic Direct Simple Shear Tests (CDSS)

A total of 77 CDSS tests were performed on reconstituted soil samples. The automatic dry funnel deposition method was used to form specimens in cylindrical split molds. More details about automatic dry funnel deposition method such as specially designed aluminum funnel, computer-controlled motor, raising speeds, etc. can be found in [45, 46]. It should be reminded that dry funnel deposition (manual method) has been widely used in various experimental studies on liquefaction [19–21, 39, 47–51]. Deposited simple shear specimens in this study typically had about 20 mm initial height and 64 mm diameter. Teflon-coated rings were stacked around a typical latex membrane to provide lateral confinement during testing. Previous literature has shown that the distribution of silt and sand fractions

within the specimen volume is reasonably uniform after being deposited by the dry funnel technique (i.e. segregation of fine and coarse grain fractions is not a concern) [21, 47, 52, 53].

All specimens were consolidated to σ'_{vc} (vertical effective stress) of 100kPa. At the cyclic loading stage, constant volume conditions (equivalent to undrained cyclic loading) of the specimens were maintained by computer control such that the height of specimens were kept constant. This is done by adjusting (i.e. increasing or decreasing) the amount of vertical stress acting on the specimens depending on their volume change tendency. The constant volume CDSS system in this study does not need any pore pressure, because drainage was not controlled. Excess pore-water pressures generated in an equivalent undrained test were predicted from the change of vertical effective stress [53]. Accordingly, an increase in vertical stress ($+\Delta\sigma_v$) to maintain constant volume conditions matches the negative excess pore pressure change ($-\Delta u_e$) in a truly undrained test (i.e., $+\Delta\sigma_v=-\Delta_{ue}$). Excess pore-water pressures predicted from a constant volume DSS test are shown to be the same as the pore pressures measured in a truly undrained DSS test [54]

Another important issue for the liquefaction experiments and relevant investigations in the laboratory is the degree of saturation. Finn and Vaid [55] investigated the cyclic liquefaction behavior of Ottawa sand via dry and saturated specimens under constant volume direct simple shear loading and reported an identical response for dry and saturated specimens. This finding was important because it indicates that dry specimens can be used to study the clean sand behavior in undrained conditions. Later, Monkul et al. [56] performed constant volume CDSS tests and compared the liquefaction behavior of specimens in dry and saturated conditions. According to their results, the cyclic liquefaction response of silty sands (i.e. with non-plastic silt only) and clean sands can be determined by using dry specimens under constant volume CDSS loading. Recently, Monkul et al. [57] also tested non-plastic silts in constant volume DSS tests and obtained their monotonic undrained shear strength from dry specimens. There are other studies in which dry specimens were tested in constant volume CDSS tests [58–60]. To benefit the inherent capacity of the constant volume CDSS system explained above and to exclude the demanding saturation process, all the simple shear specimens in this investigation were tested in a dry condition by constant volume CDSS loading.

Shear stresses (τ_{cy}) were applied in a uniform manner at four cyclic stress ratios (i.e. CSR = τ_{cy}/σ'_{vc}=0.1, 0.12, 0.14, and 0.18) at 0.1 Hz frequency during cyclic loading. When the predicted excess pore water pressure of the samples becomes equal to the initial vertical effective stress of 100kPa liquefaction is considered to occur. Cyclic loading continued until the specimens either liquefied (i.e., $r_u = \Delta u_e/\sigma'_{vc}$=1) or 10% double amplitude (D.A.) shear strain was reached. It should be noted that the influence of the two alternative failure criteria (i.e., 10% D.A. shear strain and r_u=1) on the results is not significant, because the average r_u value for the specimens at which double amplitude shear strain condition governed was also calculated to be close to 1 (i.e. 0.93). As can be seen in Fig. 3a-b, which show CDSS response for a silty sand specimen, the occurrence of two alternative failure conditions (i.e., r_u=1 and 10% D.A. shear strain) is quite close to each other.

3.2 Seismic Cone Penetration and Direct Push Permeability Tests

A group of 13 tests—CPTu, SCPTu, and DPP—were performed on clean and silty sands mentioned before. Summary of the prepared samples and test results are presented in Table 2. Each soil was deposited into a rigid-walled box which would result specimens with a width of 45 cm, a length of 163 cm, and an initial height of 144 cm. For the sample preparation, the dry pluviation method was used, which is equivalent to the method used in the previously explained CDSS tests. For this approach, dry soil is deposited directly through a large funnel into the box to minimize particle segregation of silty sands [62] as well as to be consistent with the fabric of simple shear specimens. Once the dry soil reached a depth of 144 cm, carbon dioxide was evenly introduced into the specimen for about one hour, from the bottom of the box towards the top, in order to remove the air inside the specimen. Then, the water was allowed to flow after the percolation of carbon dioxide. For each sample, the relative density is evaluated in two ways. The first one is based on the dry weight of each sample and the amount of water added to the sample by using relevant phase relationships. With this method, the average D_r was obtained for each sample. The second one is by using the relationship between k and D_r, as demonstrated in Fig. 2b, based on the measured k of specimens by DPPT tests, which will be further explained in the following sections. With this method, D_r values were obtained at specific depths where DPPT tests were conducted. As shown in Table 2, the D_r based on the water content and the relationship between k and D_r are tabulated in columns 7 and 8, respectively. For example, the relative density of sample S1 was determined 21–29% throughout the depth, with an average for the whole deposit close to 26%. For this sample, the average relative density obtained based on the water content was 27% which is in good agreement with the relative density range (and its average) estimated from the relationship between k and D_r. As it is important to obtain relative density at specific depths in the box, the D_r values that are listed at column 8 are used in the further analyses. More details about the sample saturation methodology and preparation process of large samples are detailed in Arik [63].

Figure 4 displays the testing setup and side view of test locations. The probe used in the piezocone penetration test was a classic cone with a tip angle of 60° and a diameter of 35.7 mm. The CPTu tests were conducted with different penetration rates, from 0.8 cm/sec to 1.5 cm/sec. The cone penetration rates, as well as the measured cone penetration resistance (q_c) and pore water pressure (u_2) values, are tabulated in Table 2. The recorded penetration resistance was normalized as shown below [64]:

$$q_{cIN}=\frac{q_c-\sigma_{vo}}{(\sigma_{vo}')^c} \quad (1)$$

$$c=1-(D_r-10\%)-0.007 \quad (2)$$

Here, σ_{vo}' is the effective vertical stress, σ_{vo} is the total vertical stress and q_c is the measured cone resistance in atm units. c is the stress normalization exponent, which was estimated from Eq. 2, proposed by Olsen [64]. In this study, the c values changed from 0.58 to 0.92 for D_r of 70–21%, respectively.

One of the most important factors affecting the CPTu measurements in the box is the ratio of the diameter of the box to the CPTu probe ($R_d=D_c/d$). Several researchers [65–67] have studied the effects of boundary conditions on CPTu data. Parkin and Lunne [65] reported that for loose soil, the side boundary effects are negligible. Phillips and Valsangkar [66] and Renzi et al. [67] stated that for dense soil, the side boundary effects are not significant even for R_d = 11. In this study, CPTu tests were performed along one concentric circle that has a diameter of 45 cm. The cone that has a diameter of 3.57 cm gives a R_d value of 13. In view of the above, the boundary conditions of the box can satisfactorily model the in-situ free field conditions when the R_d values revealed in the literature are examined.

Following the CPTu tests, seismic CPTu tests (SCPTu) were performed, based on ASTM D5778-12 [68] standards. As shown in Fig. 4, the SCPTu was performed 0.8 m apart from the CPTu testing hole. The S-plate was placed on the soil sample surface 1 m apart from the SCPTu hole. The horizontal shear waves were generated by hitting the S-plate laterally with a sledgehammer. The S-waves were then transmitted through the soil and reached the seismometer at the seismic rod. The measured V_s values are listed in Table 2 (column 5) and these results were used to derive the coefficient of volume compressibility of the soils (m_v) as shown in Eq. 3 below:

$$m_v = \frac{1.5(1-2\nu)}{V_s^2 \rho(1+\nu)} \qquad (3)$$

Here, ρ is the density of the soil, and v is the Poisson's ratio. Precise v measurement is very difficult due to the bedding errors and system compliance in the laboratory [69, 70]. Therefore, the results of Suwal and Kuwano [71] were used to evaluate the v of silty sands in fully saturated conditions. Poisson's ratio values for each FC are given in Table 2.

Following the SCPTu test, permeability was obtained by DPPT at the same depth intervals the SCPTu tests were completed. Figure 4 shows the DPPT testing location. As shown in Fig. 5, a complete DPPT testing tool used in the laboratory contains a cylinder water tank with valve attachment points for water and compressed nitrogen gas, a probe with a 60° tip angle and a 3.57 cm diameter, and a perforated screen with a slit size of 0.3 mm and a length of 45 mm. During the DPPT, the water was first filled inside the cylinder tank specifically designed for the DPPT setup, and then it was rapidly pressurized via compressed nitrogen gas. The flow speed of the water from the perforated screen was then measured as water discharged into the soil over a measured time and pressure. The applied excess head (Δh) and the measured volumetric flow (Q) were used to find the permeability of each sample at distinct depths, as shown below [72]:

$$k = \frac{Q}{4\pi . \Delta h . a_s}$$

4

where, a_s represents the spherical injection region radius, which was 1.44 cm in this study. During the tests, drainage is only allowed from the top of the soil samples.

4. The Role Of Fines On Cpt Resistance - Crr Correlation

4.1 Effect of Fines and Relative Density on Excess Pore Pressure and CPT Resistance

CPTu test data were used to demonstrate the relationship between relative density and normalized penetration resistance, as well as the relationship between relative density and excess pore water pressure for sand having different FCs. Figure 6a shows the relationship between excess pore water pressure ratio and D_r for the same soils (i.e. FC between 0% and 35%) based on CPTu tests. It is clear that at each fines content, the excess pore water pressure ratio decreases with an increase in D_r. However, at a given relative density, no clear relationship existed between the excess pore water pressure ratio and FC, as the trend curves cross each other. The low confinement stress is clearly contributing to the observed behavior and resulted in enhanced dilation.

Figure 6b illustrates the effect of FC and D_r on the normalized cone penetration resistance data which corresponds with four different FCs. It is clear that at a specified relative density, the q_{c1N} decreased, with an increase in FC from 0 to 35%. For each FC, the CPT resistance increased with an increase in relative density, where the general trend of increase was represented by solid trend curves having exponential functions, seen in Fig. 6b. A change in the relative density of clean sand (FC = 0%) from 20–40% (within loose state) and from 40 to 60% (within medium dense state) increased the q_{c1N} by a factor of about 2.1. For silty sand having 5% and 15% silt, the increase in normalized CPT resistance is almost similar to the increase in clean sand. For silty sand having 35% silt, with an increase in relative density, the normalized cone tip resistance increased more subtly as compared with a lower percentage of silt. A change in relative density of silty sand (containing 35% fines) from 50–75% (medium dense to dense state) increased the normalized CPT resistance by a factor of 1.8.

The relationships between CPT resistance and D_r of clean sand and silty sand having 15% and 35%, determined in this study, are also compared in Fig. 7a with the dashed curves given by Cubrinovski [73]. As shown in the figure, there is a similar trend between q_{c1N} and D_r at FC of 0% and 15%. However, for 35% FC, at a given relative density, the q_{c1N} values developed by Cubrinovski [73] are slightly higher than the ones developed in this study.

4.2 Effect of Fines and Relative Density on CRR

As mentioned before, CDSS tests in this study were performed through a wide range of relative density values on various clean and silty sand specimens, which had different FCs (0%, 5%, 15%, and 35%). The liquefaction resistance of clean and silty sand specimens were compared with $(CRR)_{N=20}$. According to Ishihara [48], 20 uniform loading cycles could be used to determine the liquefaction resistance of laboratory specimens, based on the typical number of significant cycles in many past earthquakes. Hence, in this study, $(CRR)_{N=20}$ is considered as the cyclic stress ratio required to cause liquefaction of specimens in 20 uniform cycles.

For determining the $(CRR)_{N=20}$ of different silty sands, the number of cycles to liquefaction (N_L) versus CSR data were plotted on a semi-logarithmic graph for different relative density values. Then, corresponding $(CRR)_{N=20}$ values were determined at N_L=20 for different soil samples. Figure 7b shows the change of liquefaction resistance with relative density and FC. As expected, $(CRR)_{N=20}$ increases alongside D_r for all samples—as seen in Fig. 7b—and there is a linear relationship between $(CRR)_{N=20}$ and D_r for the studied range. In several previous studies, such linear relationships have also been observed for other soils [18, 74, 75].

The influence of FC on the $(CRR)_{N=20}$ of silica sand seems to be complicated. Still, based on Fig. 7b, one can make general observations. Adding 5% silt to the base sand increased its cyclic strength compared to the clean sand (FC = 0%) at a given relative density; however, the level of influence decreased as the soil became looser (i.e., D_r decreased). Further addition of fines from 5–15% and from 15–35% had systematically decreased $(CRR)_{N=20}$ at a given D_r (trend lines shifted downwards). One can also observe that the clean sand curve is crossed by the 15% silty sand curve around D_r of 45%, which adds complexity to the FC's effect on liquefaction resistance. Similar crossings of $(CRR)_{N=20}$ curves for different silty sands could be seen in literature [5, 18], as well as discussed in detail by Tutuncu et al. [75].

4.3 Effect of Fines on CPT Resistance - CRR Correlation

Two relationships were obtained from the laboratory tests conducted with the sand-silt mixtures. The first relationship described briefly before, is between $(CRR)_{N=20}$ and D_r for clean and silty sands having different FC (Fig. 7b). A correction factor (0.9) proposed by Seed et al. [76] was applied to the results of the CDSS tests to account for the multi-directional shaking during an earthquake (i.e. N = 20 relates to the M_w8.0). Moreover, to obtain M_w7.5, a magnitude scaling factor of 0.83 was applied to the results of the CDSS tests. The second relationship is between q_{c1N} and D_r for the same clean and silty sands having various FC values obtained from CPTu and DPPT tests (Fig. 6b). These two relationships, via common D_r values, were combined to obtain the $(CRR)_{7.5}$ versus q_{c1N} for various ranges of FCs, as shown in Fig. 8. For relative density less than 70%, the measured q_{c1N} values range from 10 to 125, and the proposed solid curves for each FC fall below a $(CRR)_{7.5}$ of 0.23. At high q_{c1N} values, the measured data were relatively limited. However, it should be emphasized that the studied q_{c1N} range in this study (< 150) is

one of the most critical regions in the CPT-based assessment charts due to the high potential of liquefaction, yet the previous research investigating the liquefaction behavior through this region was also quite limited.

Figure 8 shows that the data points for q_{c1N} less than about 25 were bundled together for sands in this study regardless of the FC. As FC increases from 0–5%, there is an obvious increase in $(CRR)_{7.5}$ at a given q_{c1N} value over 25. With further increase in FC from 5–15% had relatively increased $CRR_{7.5}$ at a given q_{c1N}. For the sand with 35% FC, a sharp increase is observed in $CRR_{7.5}$ with increasing q_{c1N}, however, the q_{c1N} data is limited (< 30). As displayed in the figure $CRR_{7.5}$ increases relatively more rapidly with q_{c1N}. Moreover, the available experimental data incorporating both controlled in-situ and laboratory tests at this region is extremely limited in the literature.

5. The Role Of The Normalized Penetration Rate On Cpt Resistance - Crr Correlation

The findings above indicate that the simplified liquefaction methods should be used with caution. Successful usage of these charts at different drainage conditions could also be considered for better representation of the liquefaction assessments. During the penetration of a cone into saturated sand or silty sand, the penetration causes loads and shear strains on the soil around the cone. The shear strains and the excess pore water pressures around the cone are highly non-uniform. Therefore, depending on the rate of penetration (v), the diameter of the penetrating object (d), and consolidation characteristics of the soil (c_h), dissipation of excess pore pressures and consolidation may vary around the cone. For a more accurate assessment of the liquefaction resistance based on the CPT test, there is a clear need for a CRR–q_{c1N} correlation based on c_h of the soil, cone penetration rate, and diameter of the cone during penetration. Relatively recently, c_h, v, and d were combined to introduce a non-dimensional penetration rate (T), as follows [33, 34]:

$$T=\frac{v\,d}{c_h} \tag{5}$$

The c_h of the silty sands plays a primary role in pore water pressure dissipation during cone penetration. Therefore, first, a closer investigation is needed to assess the effect of FC and relative density on c_h. At different FCs, Fig. 9 shows the variation of c_h with various D_r. The c_h of the prepared samples in the box was calculated by Eq. 6 given below:

$$c_h=\frac{k}{m_v\gamma_w} \tag{6}$$

where, γ_w is the unit weight of water, and m_v (Eq. 3) and k (Eq. 4) were derived from the SCPTu test and DPPT test data, respectively. Therefore, the c_h data given in the figure are calculated at depths where SCPTu and DPPT tests were performed. In the figure, the D_r values were obtained by combing the permeability measured by DPPT at each test, as well as the k versus D_r at each FC indicated in Fig. 2b.

As shown in Fig. 9, because of the reduction in permeability when increasing the silt content, the magnitude of c_h also decreases by about two orders of magnitude when the silt content increases to 15%, compared to the c_h of the clean sand. Moreover, the c_h of silty sand with 5% fines is practically not different from that of the clean sand. However, as seen in the figure, the c_h of silty sands with 15% and 35% fines is considerably different from clean sand, when compared at the same D_r. The c_h of silty sand with 15% and 35% fines are much smaller than the c_h of clean sand. The difference of c_h between clean sand and silty sands would lead to the variation of dissipation time of induced excess pore water pressure generated as the cone penetrates through the soil. This is quite important because it would result from different drainage conditions in clean and silty sands having different FC and such differences in drainage conditions should be expected to play an important role in the measured cone resistances.

5.1 Effect of Normalized Penetration Rate on Excess Pore Pressure and CPT Resistance

It is expected that the excess pore water pressure and cone penetration resistance differ in soils due to the variations in permeability and non-soil-property-related parameters, such as v and d. In the experiments, the diameter of the cone (35.7 mm) was constant. Hence, T is controlled by the c_h (varied from 1 cm^2/sec to 10^3 cm^2/sec), and v (varied from 0.8 cm/sec ~ 1.5 cm/sec). Several researchers used T to examine the effect of penetration rates on clean sand and sand with different silt contents [77–79]. The maximum penetration velocity applied in their CPT tests was not large enough to trigger the transformation from drained to partially-drained, or even to undrained conditions. Hence, to have a wide range of T values to trigger transformation from drained to partially-drained, or even to undrained conditions, authors slightly changed the penetration velocity which is close to the penetration rate applied in standard CPT tests (2 cm/sec).

The above given experimental results are presented in Figs. 10a-b in terms of $\Delta u/\sigma_{vo}'$ versus T and q_{c1N} versus T at different relative densities of the clean and silty sands. In each figure, the data points are obtained for three distinct ranges of relative densities ($20\% < D_r \leq 30\%$, $45\% \leq D_r < 60\%$, and $60\% \leq D_r < 70\%$). The corresponding green shaded area in the figure represents the relative density range from 20–30%. The gray area signifies the relative density between 45% and 60%, and the pinkish shaded area represents the relative density from 60 to 70%. Other relevant information of the data points plotted in Figs. 10a-b (such as fines contents, penetration depths, etc.) could be seen in Table 2 based on D_r and T values of the points.

Figure 10a shows the relation between $\Delta u/\sigma_{vo}'$ behind the cone tip and T for the clean and silty sands with different relative densities. The $\Delta u/\sigma_{vo}'$ remains very small for all soils when $T < 0.01$, which could be assumed as a drained condition. At $T > 0.01$, $\Delta u/\sigma_{vo}'$ increases at $D_r \leq 30\%$, while $\Delta u/\sigma_{vo}'$ decreases at $D_r \geq 60\%$. Such trends are in accordance with the basic principles of volume change behavior of soils. For instance, for dense states (i.e. $D_r \geq 60\%$), as T increases, a considerable amount of negative $\Delta u/\sigma_{vo}'$ develops, which indicates the dilative behavior of the dense soil under cone penetration. Meanwhile, there is a transition behavior from increasing $\Delta u/\sigma_{vo}'$ to decreasing $\Delta u/\sigma_{vo}'$ between 45–60% relative density.

The change in T and D_r also effects the cone penetration resistance. The observations from Fig. 10b imply that at a given relative density, the q_{c1N} of a larger T would be smaller than that of a smaller T. A reduction of q_{c1N} is seen in the soil with an increase in T, which can be attributed to the difference in FC (leading to different k and c_h) and penetration velocity. Regarding the fines content effect, as mentioned before c_h decreases with increasing FC at a given D_r (Fig. 9). Hence, for the same d and v, the T increases with increasing FC (Eq. 5) at a given D_r. Therefore, the effect of FC was inherently reflected in Fig. 10b. Due to the change in the coefficient of the consolidation and penetration rate, the change of the normalized penetration rate was investigated from about T = 0.001 to about T = 5. For each relative density, normalized penetration resistance values are high at low T values (from 0.001 to 0.01). This can cause high effective stress around the cone tip due to the shorter dissipation time of pore water pressure, representing a drained condition. The increase of T from 0.01 to about 5 caused normalized penetration resistance to decrease significantly, representing the partially drained condition. The increase of T from 5 changed normalized penetration resistance in minimal values, representing an almost-undrained condition. A higher T value can cause lower effective stress around the cone tip due to the longer dissipation time of pore water pressure.

The findings of this study align with the related research conducted by several researchers [37, 80–82]. For example, Ecemis [37] found the limiting value of T for drained and undrained conditions between 0.01 and 6, respectively. In the same line, based on the studies of Schneider et al. [80], the partially drained condition was at intermediate T values of about 0.03 to 10. Doan and Lehane [82] suggested partially-drained penetration at 0.01 to 7. Similar experimental observations were also reported in clayey soil by Jaeger et al. [81], in which the limiting valued T for drained and undrained conditions was 0.01 and 20, respectively.

The effect of permeability, the penetration rate, and the diameter of the cone on q_{c1N} and pore water pressure ($\Delta u/\sigma_{vo}'$) at different D_r values agrees favorably with one another once they are normalized to the same T value. So, it can be inferred that T would be a more reasonable parameter than the fines content of the soils to quantify the degree of consolidation during cone penetration.

5.2 Effect of the Normalized Penetration Rate on CPT Resistance – CRR Correlations

Two relationships were combined to obtain the $(CRR)_{7.5}$ versus q_{c1N} for different ranges of T values. The first relationship is between $(CRR)_{7.5}$ and T at different relative density ranges. $(CRR)_{7.5}$ and T relationship is obtained by combining, $(CRR)_{N=20}$-D_r (Fig. 7b) and c_h-D_r (Fig. 9) for clean and silty sands having different FC. The second relationship is between q_{c1N} and T (Fig. 10b) at different relative density ranges.

Figure 11a shows the $(CRR)_{7.5}$ versus q_{c1N} for two distinct ranges of normalized penetration rates. These results are grouped for two sets of T values (a) $0.001 < T < 0.01$ and (b) $0.5 < T < 5$. The corresponding upper and lower limit values of the T values are represented by the curves. The T values less than 0.01 correspond to a drained condition, whereas the T values more than 5 correspond to an undrained condition as explained in Fig. 10b before. Accordingly, one should expect a transition from drained condition to undrained condition for T values between 0.01 to 5. Figure 11a clearly shows that, as T increases (which is attributed to a decrease in k and c_h and an increase in v) from 0.001 to 5, the liquefaction resistance of soils significantly increases when compared at the same q_{c1N}. Similar to the q_{c1N}-$(CRR)_{7.5}$ variation with FC, the data points corresponding to different T ranges are bundled together for q_{c1N} values smaller than 30 (i.e. the boundary curves became somewhat unclear/cross each other).

Figure 11b depicts the relationship, along with the field-based relationship, for $(CRR)_{7.5}$ versus q_{c1N} and FC, corresponding to nearly clean sand ($FC < 5\%$), silty sands at nearly 15% silt content, and 35% silt content as recommended by Robertson and Wride [25]. As mentioned earlier, these curves are widely used in practice for the evaluation of liquefaction resistance based on CPT resistance with FCs from 0–35%. Additionally, a clean sand curve that was proposed by Krage and DeJong [83] was plotted in the figure. It is interesting to observe in Fig. 11b that the T boundary line less than 0.01 follow the curves of Robertson and Wride [25] and Krage and DeJong [83] in a reasonably close manner for $FC \leq 5\%$ and clean sand, respectively. Hence, the proposed curves are consistent with the observed data shown in the figure, as FC less than 5% and clean sand represent the drained condition [84]. The Robertson and Wride [25] curves for 15% and 35% silt content also tends to be in good agreement with the results of this study and falls on the boundary line corresponding to T = 0.5 and T = 5, respectively. The increase of T from 0.01 to about 5 represents the partially drained condition. Consequently, the proposed curves representing different T values are consistent with field observations shown in the figure, as T more than 5 represents the almost-undrained condition.

The results clearly show that for a more accurate assessment of the liquefaction resistance based on the CPT test, the CRR–q_{c1N} correlations based on the coefficient of consolidation of the soil, cone penetration rate, and diameter of the cone during penetration are needed. It should also be reminded that such an approach also inherently considers the effect of FC on the liquefaction resistance of sands.

6. Summary And Conclusion

Based on an extensive experimental program, which involves several different types of experiments including cyclic direct simple shear tests, constant and falling head permeability tests, piezocone

penetration tests, seismic CPTu tests, and direct push permeability tests, a normalized penetration rate-dependent liquefaction screening chart was proposed. This chart considers the effects of consolidation characteristics and the penetration rates on cone penetration resistance on clean and non/low plastic silty sands. The following results were determined:

1. Soil having different permeability and coefficient of consolidation experience different drainage conditions, and this can cause different penetration resistance and excess pore water pressure around the cone tip. Cone resistance is sensitive to penetration rate and cone diameter, as well as k and c_h. In this study, normalized cone penetration resistance is correlated with relative density and a non-dimensional parameter T. It is found that the effect of permeability, the penetration rate, and the diameter of the cone on q_{c1N} and excess pore water pressure ratio ($\Delta u/\sigma_{vo}'$) at different D_r agrees favorably with one another once they are normalized to the same T value. Therefore, T can be used to demarcate the drained, partially-drained, and undrained conditions throughout cone penetration-based liquefaction assessments. From the experimental tests performed in this study, it was determined that the limit T value from drained to partially-drained conditions was 0.01 and partially-drained to undrained conditions around 5 during the advancement of the cone penetrometer. So, it can be inferred that T which is influenced by the coefficient of consolidation during penetration would be a more reasonable parameter than the FC of the soils to be utilized in liquefaction assessment of silty sands.
2. At very high T values (low coefficient of consolidation) silty sand contributes to a slow rate of dissipation of excess pore pressures in the soil during cone penetration, leading to smaller effective stress at the tip of a cone (nearly undrained response) when compared with the behavior of silty sand having lower T values (higher coefficient of consolidation) through a wide range of relative densities investigated in this study (i.e. $20\% < D_r \leq 70\%$) (Figs. 10a-b). This is due to the fact that the c_h of the soil decreased along with an increase in FC up to 35% (Fig. 9), indicating that employing T would also inherently involve the FC influence on liquefaction resistance.
3. The CRR-q_{c1N} relationship determined from the laboratory was proposed for ranges of T values (Fig. 11a). It has been observed that field liquefaction resistance increased as T increased (which is attributed to a decrease in k and c_h and an increase in the penetration rate) from 0.001 to 5, for each q_{c1N} value. Although the T-dependent q_{c1N}-CRR relationship depicts the same trend as observed in the field-based liquefaction screening procedures, additional studies are required to verify and refine this trend, using penetration tests in large-scale soil models.

Declarations

- *The authors declare that no funds, grants, or other support were received during the preparation of this manuscript.*
- *The authors have no relevant financial or non-financial interests to disclose.*
- *All authors contributed to the study conception and design. All authors read and approved the final manuscript."*

- *The datasets generated during and/or analyzed during the current study are available from the corresponding author on reasonable request.*

References

[1] Boulanger RW, Idriss IM. Liquefaction Susceptibility Criteria for Silts and Clays. J Geotech Geoenviron Eng ASCE 2006;132(11):1413–26.

[2] Bray JD, Sancio RB. Assessment of the Liquefaction Susceptibility of Fine-Grained Soils. J Geotech Geoenviron Eng ASCE 2006;132(9):1165–77.

[3] Boominathan A, Rangaswamy K, Rajagopal. Effect of non-plastic fines on liquefaction resistance of Gujarat sand. International J of Geotech Eng 2010;4(2):241–53.

[4] Erten D, Maher MH. Cyclic unp behavior of silty sand. Soil Dynam Earthq Eng 1995;14(2):115–123.

[5] Oka LG, Dewoolkar M, Olson SM. Comparing laboratory-based liquefaction resistance of a sand with non-plastic fines with shear wave velocity-based field case histories. Soil Dynam Earthq Eng 2018;113:162–173.

[6] Papadopoulou A, Tika T. The effect of fines on critical state and liquefaction resistance characteristics of non-plastic silty sands. Soils Found 2008;48(5):713–25.

[7] Porcino DD, Diano V. The influence of non-plastic fines on pore water pressure generation and undrained shear strength of sand-silt mixtures. Soil Dynam Earthq Eng 2017;101:311–21.

[8] Sitharam TG, Dash HK. Effect of non-plastic fines on cyclic behaviour of sandy soils. GeoCongress 2008:Geosustainability and Geohazard Mitigation, Geotechnical Special Publication ASCE 2008;178:319–26.

[9] Wang Y, Wang Y. Study of effects of fines content on liquefaction properties of sand. GeoShanghai International Conference, Geotechnical Special Publication ASCE 2010;201:272–77.

[10] Xenaki VC, Athanasopoulos GA. Liquefaction resistance of sand-silt mixtures: An experimental investigation of the effect of fines. Soil Dynam Earthq Eng 2003;23(3):183–94.

[11] Amini F, Qi GZ. Liquefaction testing of stratified silty sands. J Geotech Geoenviron Eng ASCE 2000;126(3):208–17.

[12] Hazirbaba K, Rathje EM. Pore Pressure Generation of Silty Sands due to Induced Cyclic Shear Strains. J Geotech Geoenviron Eng ASCE 2009;135:1892–1905.

[13] Shen CK, Vrymoed JL, Uyeno CK. The effect of fines on liquefaction of sands. Proceedings of the 9th International Conference on Soil Mechanics and Foundation Eng 1977:381–85.

[14] Carraro JAH, Bandini P, Salgado R. Liquefaction Resistance of Clean and Nonplastic Silty Sands Based on Cone Penetration Resistance. J Geotech Geoenviron Eng ASCE 2003;129(11):965–76.

[15] Polito CP, Martin JR. Effects of nonplastic fines on the liquefaction of sands. J Geotech Geoenviron Eng ASCE 2001;127(5):408–15.

[16] Monkul MM, Kendir SB, Tütüncü YE. Combined effect of fines content and uniformity coefficient on cyclic liquefaction resistance of silty sands. Soil Dynam Earthq Eng 2021;151:106999.

[17] Thevanayagam S. Intergrain contact density indices for granular mixes—I: Framework. Earthq Eng and Eng Vib 2007;6(2):123-134.

[18] Cubrinovski M, Rees S, Bowman E. Chapter 6: Effects of non-plastic fines on liquefaction resistance of sandy soils. Earthquake Engineering in Europe, M. Garevski and A. Ansal, eds., Springer 2010:125–144.

[19] Monkul MM, Yamamuro JA. Influence of silt size and content on liquefaction behavior of sands. Can Geotech J 2011;48(6):931–42.

[20] Monkul MM, Etminan E, Şenol A. Influence of coefficient of uniformity and base sand gradation on static liquefaction of loose sands with silt. Soil Dynam Earthq Eng 2016;89:185–97.

[21] Eseller-Bayat E, Monkul MM, Akin O, Yenigun S. The Coupled Influence of Relative Density, CSR, Plasticity and Content of Fines on Cyclic Liquefaction Resistance of Sands. Journal of Earthquake Engineering 2019;23(6):909–29.

[22] Papadopoulou A, Tika, T. The effect of fines plasticity on monotonic undrained shear strength and liquefaction resistance of sands. Soil Dynam Earthq Eng 2016, 88:191–206.

[23] Park SS, Kim YS. Liquefaction Resistance of Sands Containing Plastic Fines with Different Plasticity. J Geotech Geoenviron Eng ASCE 2013, 139(5):825–830.

[24] Youd TL, Idriss IM, Andrus RD, Arango I, Castro G, Christian JT, Dobry R, Finn WD, Harder LF, Hynes ME, Ishihara K, Koester JP, Liao SSC, Marcuson WF, Martin GR, Mitchell JK, Moriwaki Y, Power MS, Robertson PK, Seed RB, Stokoe KH. Liquefaction resistance of soils: summary report from the 1996 NCEER and 1998 NCEER/NSF workshops on evaluation of liquefaction resistance of soil. J Geotech Geoenviron Eng ASCE 2001:817-33.

[25] Robertson PK, Wride CE. Evaluating cyclic liquefaction potential using the cone penetration test. Can Geotech J 1998;35(3):442–59.

[26] Juang CH, Yuan H, Lee D, Lin P. Simplified Cone Penetration Test-based Method for Evaluating Liquefaction Resistance of Soils. J Geotech Geoenviron Eng ASCE 2003;129(1):66-80.

[27] Huang AB, Huang YT, Ho FJ. Assessment of liquefaction potential for a silty sand in Central Western Taiwan. 16th ICSMGE, 2005;2653-57.

[28] Kokusho T, Hara T, Murahata K. Liquefaction strength of fines containing sands compared with cone resistance in triaxial specimens. Pre-Workshop Proc. 2nd Japan-US Workshop on Testing, Modelling, and Simulation in Geomechanics, 2005:280-96

[29] Moss RES, Seed RB, Kayen RE, Stewart JP, Der Kiureghian A, Cetin KO. CPT-based probabilistic and deterministic assessment of in situ seismic soil liquefaction. J Geotech Geoenviron Eng ASCE 2006;132(8):1032–51.

[30] Boulanger RW, Idriss IM. CPT and SPT based liquefaction triggering procedures. Report No. UCD/ CGM-14/01, 2014, University of California at Davis, CA

[31] Thevanayagam S, Ecemis N. Effects of permeability on liquefaction resistance and cone resistance. Geotechnical Earthquake Engineering and Soil Dynamics IV ASCE 2008.

[32] Ecemis N, Karaman M. Influence of non-/low plastic fines on cone penetration and liquefaction resistance. Engineering Geology 2014;181:48–57.

[33] House AR, Oliveira JRMS, Randolph MF. Evaluating the Coefficient of Consolidation Using Penetration Tests. Int. J. of Physical Modelling in Geotechnics 2001;1(3):17-25.

[34] Randolph MF, Hope S. Effect of cone velocity on cone resistance and excess pore pressures. Proc. Int. Sym. on Eng. Practice and Performance of Soft Deposits 2004:147-52.

[35] Chung SF, Randolph MF, Schneider JA. Effect of penetration rate on penetrometer resistance in clay. J Geotech Geoenviron Eng ASCE 2006;132(9):1188-96.

[36] Kim K, Prezzi M, Salgado R, Lee W. Effect of penetration rate on cone penetration resistance in saturated clayey soils. J Geotech Geoenviron Eng ASCE 2008;134(8):1142-53.

[37] Ecemis N. Effects of Permeability and Compressibility on Liquefaction Screening using Cone Penetration Resistance. Ph.D. Dissertation, Department of Civil Structural and Environmental Engineering, State University of New York at Buffalo, 2008:282p.

[38] ASTM D2487-06. Standard Practice for Classification of Soils for Engineering Purposes (Unified Soil Classification System), 2017.

[39] Lade PV, Liggio CDJ, Yamamuro JA. Effects of non-plastic fines on minimum and maximum void ratios of sand. Geotechnical Testing Journal 1998;21(4):336–47.

[40] Cubrinovski M, Ishihara K. Maximum and Minimum Void Ratio Characteristics of Sands. Soils Found 2002;42(6):65–78.

[41] Lade PV, Yamamuro JA, Liggio CDJ. Effects of fines content on void ratio, compressibility, and static liquefaction of silty sand. Geomechanics and Engineering 2009;1(1):1–15.

[42] Monkul MM, Etminan E, Şenol A. Coupled influence of content, gradation and shape characteristics of silts on static liquefaction of loose silty sands. Soil Dynam Earthq Eng 2017;101:12–26.

[43] Yamamuro JA, Covert KM. Monotonic and cyclic liquefaction of very loose sands with high silt content. J Geotech Geoenviron Eng ASCE 2001;127(4):314–24.

[44] ASTM D2434-19. Standard Test Method for Permeability of Granular Soils (Constant Head). West Conshohocken, PA, 2019.

[45] Monkul MM, Yenigun S, Eseller-Bayat E. Importance of Automatization on Dry Funnel Deposited Specimens for Liquefaction Testing. Geotechnical Special Publication No 293; Slope Stability and Landslides, Laboratory Testing, and In Situ Testing ASCE 2018:286–95.

[46] Monkul MM, Yenigun S. Automatic funnel control device. US Patent Application

No: 17/059; 2021. p. 502. Publication No: US 2021/0208040 A1.

[47] Bahadori H, Ghalandarzadeh A, Towhata I. Effect of Non Plastic Silt on the Anisotropic Behavior of Sand. Soils Found 2008;48(4):531–45.

[48] Ishihara K. Liquefaction and flow failure during earthquakes. Geotechnique 1993;43(3):351–415.

[49] Lade PV, Yamamuro JA. Effects of nonplastic fines on static liquefaction of sands. Can Geotech J 1997;34(6):918–28.

[50] Zlatovic S, Ishihara K. Normalized Behavior of Very Loose Non-Plastic Soils: Effects of Fabric. Soils Found 1997;37(4):47–56.

[51] Wood FM, Yamamuro JA, Lade PV. Effect of depositional method on the undrained response of silty sand. Can Geotech J 2008;45:1525–37.

[52] Yamamuro JA, Wood FM, Lade PV. Effect of depositional method on the microstructure of silty sand. Can Geotech J 2008;45(11):1538–55.

[53] Bjerrum L, Landva A. Direct simple shear tests on a Norwegian quick clay. Geotechnique 1966;16(1):1–20.

[54] Dyvik R, Berre T, Lacasse S, Raadim B. Comparison of truly undrained and constant volume direct simple shear tests. Geotechnique 1987;37(1):3–10.

[55] Finn WDL, Vaid YP. Liquefaction potential from drained constant volume cyclic simple shear tests. Proceedings of the sixth world conference on earthquake engineering 1977;2157–62.

[56] Monkul MM, Gultekin C, Gulver M, Akin O, Eseller-Bayat E. Estimation of liquefaction potential from dry and saturated sandy soils under drained constant volume cyclic simple shear loading. Soil Dynam Earthq Eng 2015;75:27–36.

[57] Monkul MM., Aydin, NG, Demirhan B, Sahin M. Undrained Shear Strength and Monotonic Behavior of Different Nonplastic Silts: Sand-Like or Clay-Like? Geotechnical Testing Journal 2020;43(3):20180147.

[58] Li Y, Yang Y, Yu H, Roberts G. Monotonic direct simple shear tests on sand under multidirectional loading. International Journal of Geomechanics 2016;17(1):1–10.

[59] Viana Da Fonseca A, Soares M, Fourie AB. Cyclic DSS tests for the evaluation of stress densification effects in liquefaction assessment. Soil Dynam Earthq Eng 2016;75:98–111.

[60] Wijewickreme D, Sriskandakumar S, Byrne P. Cyclic loading response of loose air-pluviated Fraser River sand for validation of numerical models simulating centrifuge tests. Can Geotech J 2005;42(2):550–61.

[61] ASTM D8296-19. Standard Test Method for Consolidated Undrained Cyclic Direct Simple Shear Test under Constant Volume with Load Control or Displacement Control. Annual Book of ASTM Standards, Vol. 04.09, West Conshohocken, PA., 2019.

[62] Yamamuro JA, Wood FM. Effect of depositional method on the undrained behavior and microstructure of sand with silt. Soil Dyn Earth Eng 2004;24(9–10):751–60.

[63] Arık MS. Effect of Fines Content on CPT Resistance in Silty Sands. Ms. Thesis, Izmir Institute of Technology, Turkey, 2021.

[64] Olsen RS. Normalization and Prediction of Geotechnical Properties using the Cone Penetrometer Test (CPT) Ph.D. Dissertation, University of California, Berkeley, CA. 1994.

[65] Parkin AK, Lunne T. Boundary effects in the laboratory calibration of a cone penetration for sand. 2nd European Symposium on Penetration Testing, Amsterdam: Norwegian Geotechnical Institute, 1982, 1-7.

[66] Phillips R, Valsangkar AJ. An experimental investigation of factors affecting penetration resistance in granular soils in centrifuge modelling. Technical Report, Department of Engineering, Cambridge University, 1987.

[67] Renzi R, Corte JF, Rault G, Bagge G. Cone penetration tests in the centrifuge: Experience of five laboratories. Int. Conf. Centrifuge Testing 94. A.A.Balkema, Rotterdam: International Society for Soil Mechanics and Foundation Engineering (ISSMFE), 1994,77-82

[68] ASTM D5778-12. Standard Test Method for Electronic Friction Cone and Piezocone Penetration Testing of Soils. West Conshohocken, PA, 2012.

[69] Tatsuoka, F, Shibuya S. Deformation Characteristics of Soils and Rocks from Field and Laboratory Tests. Proceedings of 9th Asian Regional Conference of SMFE, Bangkok, 1992;(2):101-170.

[70] Lo Presti D, Pallara O, Lancelotta R, Amandi M, Maniscalco R. Monotonic and cyclic loading behavior of two sands at small strains. Geotechnical Testing Journal, 1993;16(4),409-24.

[71] Suwal LP, Kuwano R. Poisson's ratio evaluation on silty and clayey sands on laboratory specimens by flat disk shaped piezo-ceramic transducer. Bulletin of ERS; 2012:45.

[72] Lee DS, Elsworth D, Hryciw R. Hydraulic conductivity measurement from on-the-fly uCPT sounding and from visCPT. J Geotech Geoenviron Eng ASCE 2008;134(12):1720–29.

[73] Cubrinovski M. Some important considerations in the engineering assessment of soil liquefaction. NZ Geomechanics News, 2019; Issue 97.

[74] Park SS, Nong ZZ, Lee DE. Effect of vertical effective and initial static shear stresses on the liquefaction resistance of sands in cyclic direct simple shear tests. Soils Found 2020;60:1588–607.

[75] Tütüncü YE, Kendir SB, Monkul MM. Influence of silt content on cyclic liquefaction of sand: conflicting effects of relative density. Proceedings of the 20th International Conference on Soil Mechanics and Geotechnical Engineering, ISSMGE, 2022.

[76] Seed HB, Martin GR, Pyke CK. Effects of multi-directional shaking on pore pressure development in sands. J Geotech Eng Div. 1978;104(1):27–44.

[77] Kumar J, Raju K. Penetration rate effect on miniature cone tip resistance for different cohesionless material. Geotech. Test. J. 2009;32(4):375-84.

[78] Kokusho T, Ito F, Nagao Y, Green AR. Influence of non/low-plastic fines and associated aging effects on liquefaction resistance. J Geotech Geoenviron Eng ASCE 2012;138(6):747–56.

[79] Oliveira JRMS., Almeida MSS., Motta HPG, Almeida MCF. Influence of penetration rate on penetrometer resistance. J Geotech Geoenviron Eng ASCE 2011;137(7):695-703.

[80] Schneider JA, Lehane BM, Schnaid F. Velocity effects on piezocone tests in normally and overconsolidated clays. Int. J. Phy. Model. Geotech. 2007;7(2):23–34.

[81] Jaeger RA, DeJong JT, Boulanger RW, Low HE, Randolph MF. Variable penetration rate CPT in an intermediate soil. In Proc., 2nd Int. Symp. on Cone Penetration Testing, 2010.

[82] Doan LV, Lehane BM. CPT data in normally consolidated soils. Acta Geotechnica; 2021:1-9.

[83] Krage CP, DeJong JT. Influence of drainage conditions during cone penetration on the estimation of engineering properties and liquefaction potential of silty and sandy soils. J Geotech Geoenviron Eng

ASCE, 2016:142.11:04016059.

[84] Gomez BW, Dewoolkar MM, Lens JE, Benda CC. Effects of Fines Content on Hydraulic Conductivity and Shear Strength of Granular Structural Backfill. Transportation Research Record. 2014;2462(1):1-6.

Tables

Tables 1 and 2 are available in the Supplementary Files Section.

Figures

Figure 1

(a) Gradation curves, and (b) SEM photo of sand-silt mixture (e.g., 15% FC) used in the experiments.

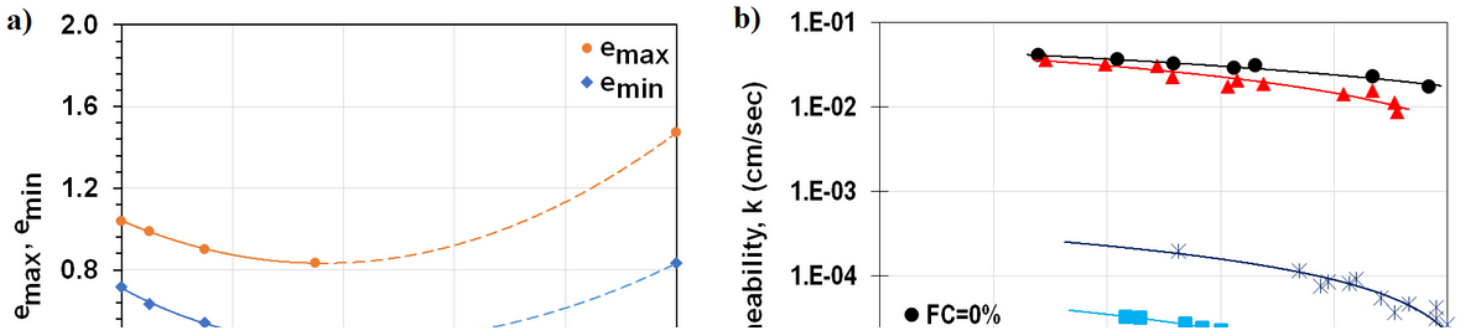

Figure 2

(a) Variation in the maximum (e_{max}) and minimum (e_{min}) void ratios of silty sands with fines content, and (b) variation of permeability with D_r at sand-silt mix of 0%, 5%, 15%, and 35% fines content.

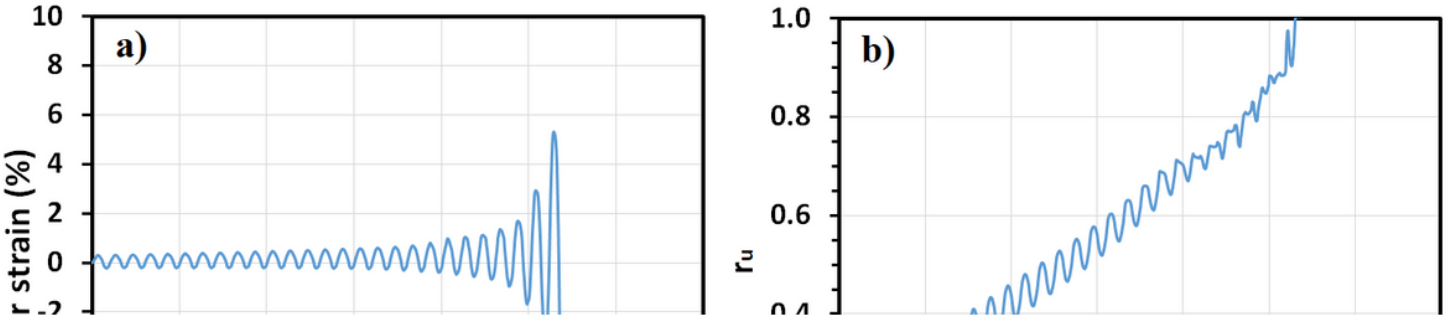

Figure 3

Typical CDSS test result of a silty sand specimen (sand with 15% silt at CSR=0.1, D_r=40.4%): a) shear strain vs. the number of cycles, and b) pore pressure ratio (ru = Δue/σ'vo) vs. the number of cycles

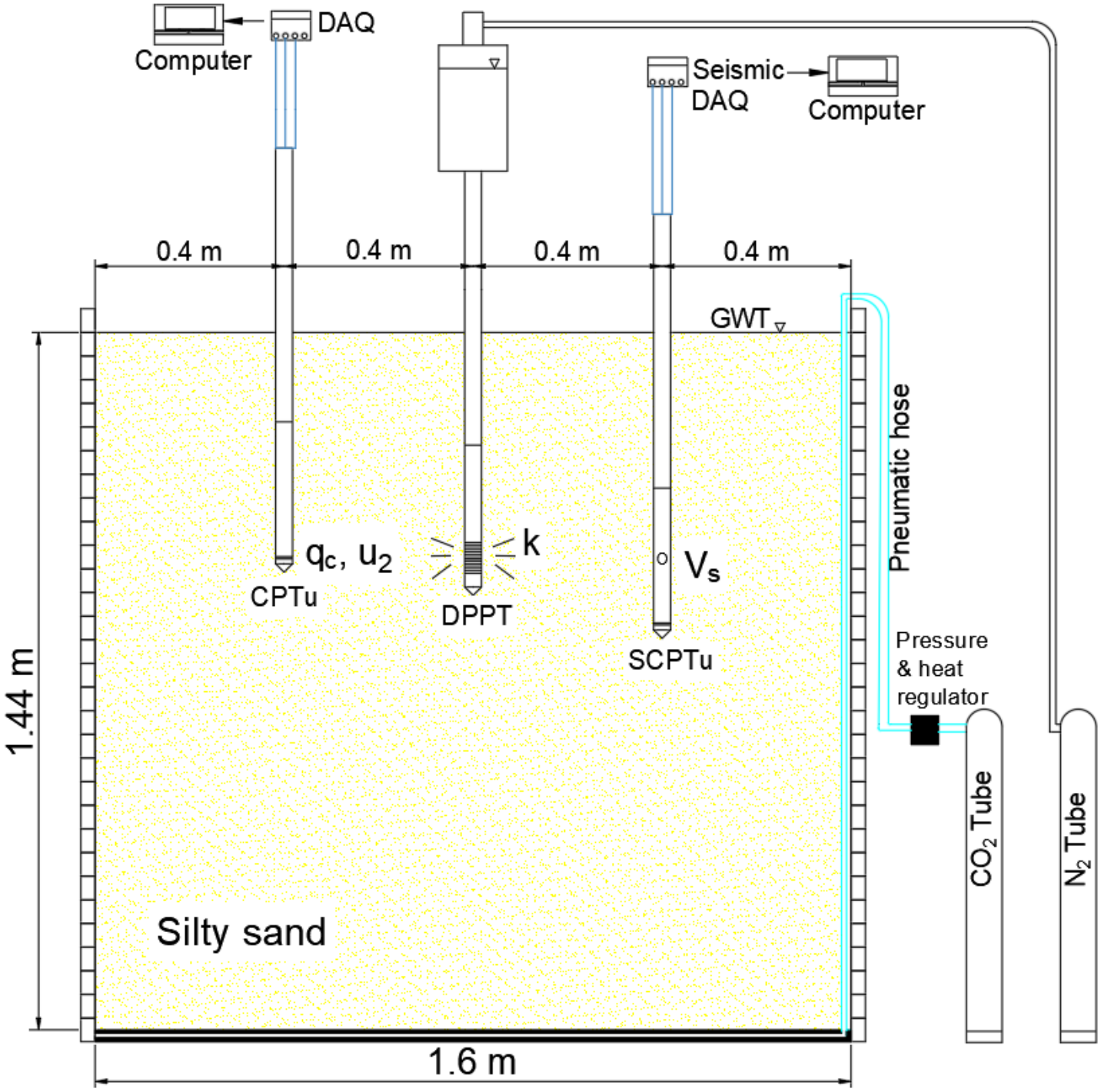

Figure 4

Schematic view of piezocone penetration (CPTu), seismic piezocone penetration (SCPTu), and direct push permeability (DPPT) tests conducted inside the box.

Figure 5

(a) Direct push permeability testing system used in the laboratory, and (b) perforated screen (slit size of 0.3 mm and length of 45 mm).

Figure 6

Experimental test results: (a) q_{c1N} versus D_r, and (b) $\Delta u/\sigma_{vo}'$ versus D_r at sand-silt mix of 0%, 5%, 15%, and 35% fines content.

Figure 7

CDSS test results: Change of$(CRR)_{CDSS}$ with D_r at sand-silt mix of 0%, 5%, 15%, and 35% fines content.

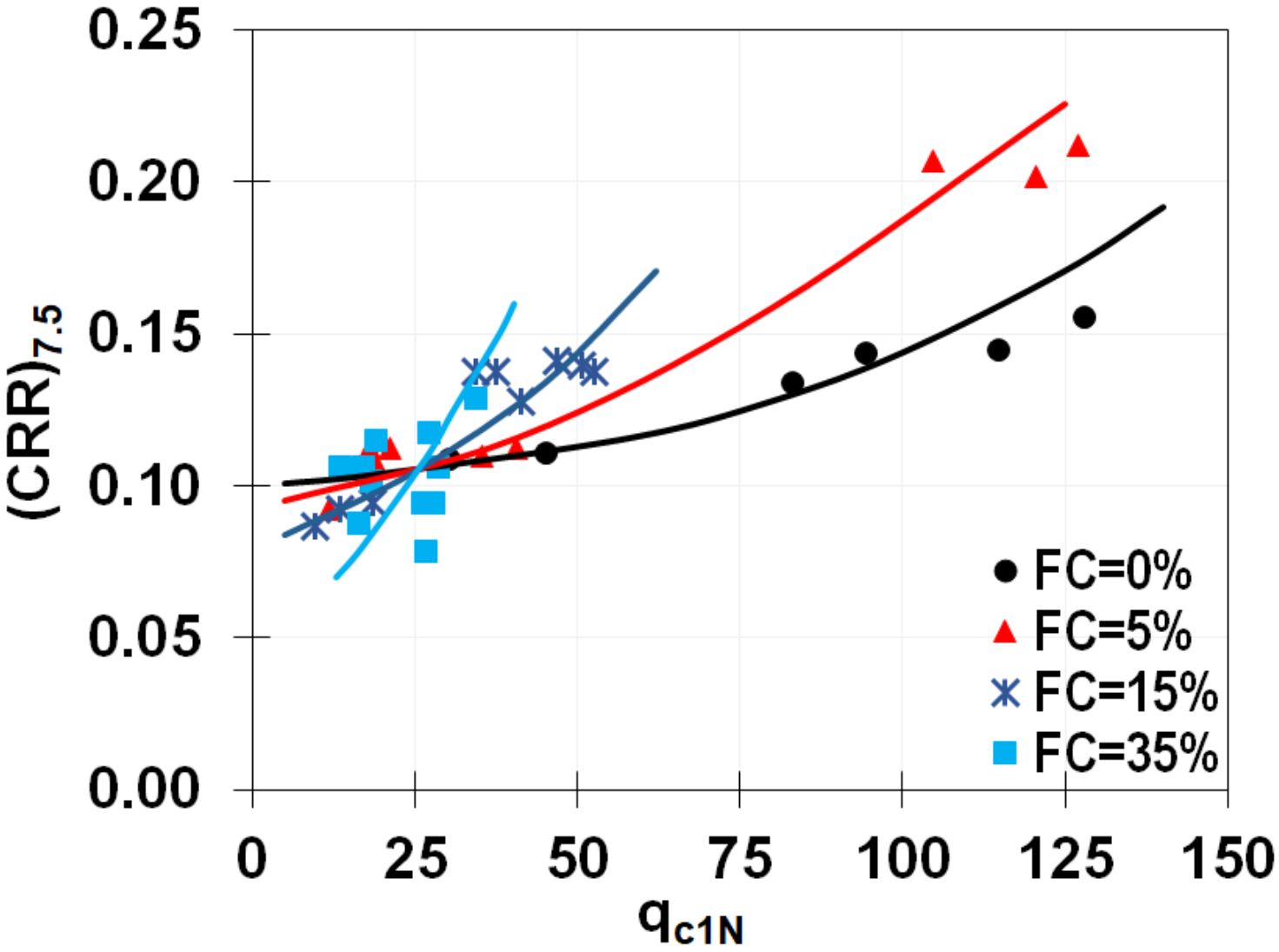

Figure 8

$(CRR)_{7.5}$-q_{c1N} relationship at sand-silt mix of 0%, 5%, 15%, and 35% fines content.

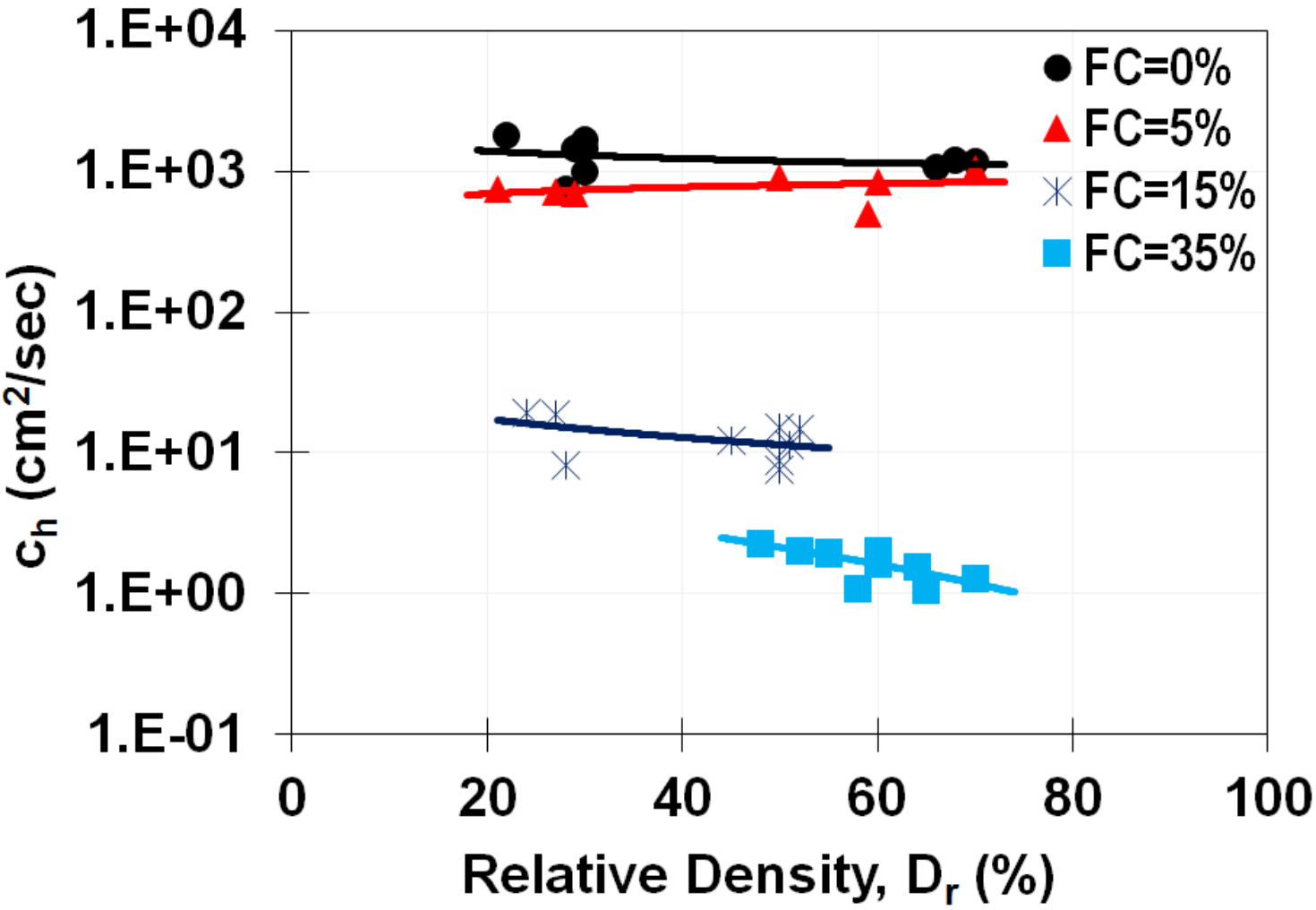

Figure 9

Variation of coefficient of consolidation with D_r at sand-silt mix of 0%, 5%, 15%, and 35% fines content.

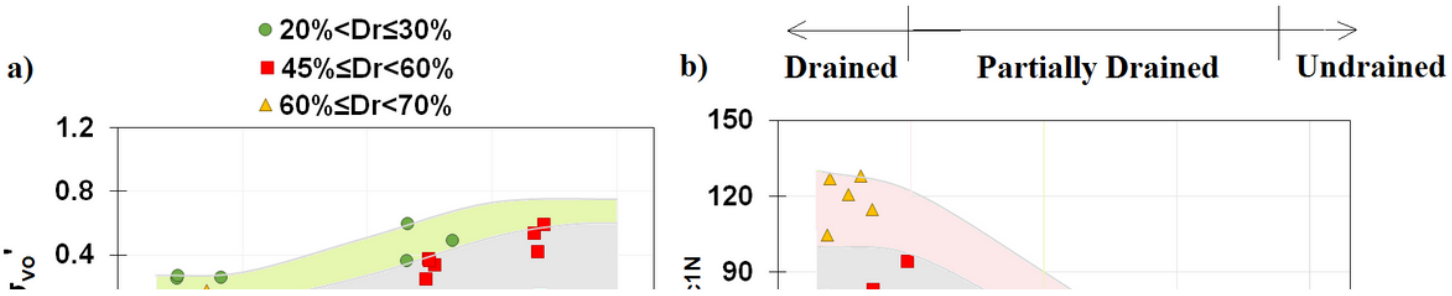

Figure 10

Effect of normalized penetration rate and $D_r$on (a) excess pore water pressure ratio, and (b) normalized cone penetration resistance of clean and silty sands at different fines content.

Figure 11

(a) $(CRR)_{7.5}$-q_{c1N}data at different normalized penetration rate ranges,and (b) curves from existing CPT-based liquefaction assessment criteria of clean sands and sands with fines.

Supplementary Files

This is a list of supplementary files associated with this preprint. Click to download.

- Table1.xlsx
- Table2.xlsx